

Optical Control of Cannabinoid Receptor 2-Mediated Ca^{2+} Release Enabled by Synthesis of Photoswitchable Probes

Roman C. Sarott, Alexander E. G. Viray, Patrick Pfaff, Anastasiia Sadybekov, Gabriela Rajic, Vsevolod Katritch, Erick M. Carreira,* and James A. Frank*

Cite This: *J. Am. Chem. Soc.* 2021, 143, 736–743

Read Online

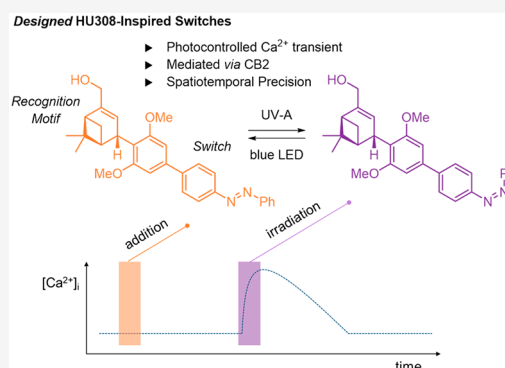
ACCESS |

Metrics & More

Article Recommendations

Supporting Information

ABSTRACT: Cannabinoid receptor 2 (CB2) is a promising target for the treatment of neuroinflammation and other diseases. However, a lack of understanding of its complex signaling in cells and tissues complicates the therapeutic exploitation of CB2 as a drug target. We show for the first time that benchmark CB2 agonist HU308 increases cytosolic Ca^{2+} levels in AtT-20(CB2) cells via CB2 and phospholipase C. The synthesis of photoswitchable derivatives of HU308 from the common building block 3-OTf-HU308 enables optical control over this pathway with spatiotemporal precision, as demonstrated in a real-time Ca^{2+} fluorescence assay. Our findings reveal a novel messenger pathway by which HU308 and its derivatives affect cellular excitability, and they demonstrate the utility of chemical photoswitches to control and monitor CB2 signaling in real-time



INTRODUCTION

The endocannabinoid system is a highly conserved lipid signaling network in all vertebrates, including humans, and is the subject of considerable research efforts aimed at its therapeutic exploitation.^{1,2} It includes two cannabinoid receptors belonging to the class A family of G protein-coupled receptors (GPCRs).^{3,4} Cannabinoid receptor 1 (CB1)⁵ is highly expressed in the central nervous system and mediates the psychotropic effects of Δ^9 -tetrahydrocannabinol (Δ^9 -THC).^{6–8} Cannabinoid receptor 2 (CB2)⁹ is best known for its role in cells of the immune system.^{8,10} Its expression and function in other cell types, tissues, and organs remain highly contested. The pharmacological regulation of CB2 holds promise for the treatment of neurodegenerative diseases, including Alzheimer's disease (AD), multiple sclerosis, and amyotrophic lateral sclerosis as well as tissue injury and inflammation.^{1,11–14} Recently, several structural studies have provided insight into CB2-ligand interactions.^{15–17}

CB2 is linked to a large number of cellular signaling pathways and exhibits pronounced biased signaling in response to different ligands.^{18,19} A functional understanding of these pathways is crucial to fully realize the receptor's therapeutic potential. Ca^{2+} ions are ubiquitous intracellular messengers in cellular signaling, and they are of emerging interest in connection with AD and other neurodegenerative diseases linked to CB2.^{20,21} Ca^{2+} is known to be released from a variety of extra- and intracellular reservoirs upon CB2 activation.^{22–24} However, the kinetics and dynamics of these pathways remain poorly studied, and deconvolution of the intricacies of these requires the design of functional chemical probes. Photo-

pharmacology, in which light is used for reversible isomerization of pharmacologically active ligands, has emerged as a prominent approach allowing researchers to manipulate signaling events in cells, tissues, and organisms with spatiotemporal precision.^{25,26} To this end, photopharmacological tools that enable dynamic control with spatial and temporal resolution over CB2-mediated Ca^{2+} signaling would open up new avenues for the field.²⁷

We previously demonstrated the first example of reversible optical control over cannabinoid receptors.^{28,29} Photoswitchable Δ^9 -THC derivatives (*azo*-THCs) showed differential, light-dependent activity at CB1 receptors and activated multiple downstream CB1 effector pathways. *Azo*-THCs reversibly targeted CB1 to potentiate inwardly rectifying K^+ channel currents and to inhibit adenylyl cyclase activity. More recently, a report by Decker and co-workers described azobenzene-substituted benzimidazoles that displayed distinct affinities toward CB2 in their *trans*- and *cis*-configurations.³⁰ However, no real-time control over CB2 signaling was demonstrated. Consequently, further studies to attain dynamic control, including the development of more advanced photoswitchable probes and assays enabling real-time visualization of GPCR activity, are required.

Received: August 19, 2020

Published: January 5, 2021



As a follow up to our work on CB1 optical control with Δ^9 -THC derivatives, we examined ligands for CB2 inspired by HU308,³¹ commonly employed as a benchmark agonist. Interestingly, over the course of our studies, we observed that HU308 stimulates intracellular Ca^{2+} -release in an AtT-20(CB2) cell line through CB2 and phospholipase C (PLC)-mediated pathways, which to the best of our knowledge has not been reported. We have leveraged these findings to devise photoswitchable HU308 azobenzene derivatives (*azo*-HU308s), which offer CB2-mediated control over intracellular Ca^{2+} upon irradiation with light. This work provides novel tools to study CB2 biology, and also highlights a novel effect of HU308 and its derivatives on CB2 effector pathways. Moreover, we utilize our findings to develop a time-resolved CB2 assay based on real-time fluorescent Ca^{2+} imaging.

RESULTS

Design, Synthesis, and Characterization of Photoswitchable HU308 Derivatives. Reported more than 20 years ago, HU308 is a privileged ligand and widely used in CB2 pharmacology owing to its high affinity and potency.¹⁹ Only recently it has been explored as a blueprint for synthetic modification, leading to chemical tools for CB2. In this regard, replacement of the allylic alcohol in HU308 with an amide linkage enabled attachment of fluorescent dyes via flexible linkers and led to highly specific imaging probes.^{32,33} A wide range of groups are tolerated at this position without affecting binding affinity. This was corroborated by docking studies, which indicated extension of reporter elements out of the orthosteric binding pocket of CB2.

Optimal photoswitches require differential biological activity of light-induced configurations. Inspection of docking poses indicated that the alkyl side chain of HU308 derivatives is embedded deeply in the binding pocket. Accordingly, we identified the 3'-position as the ideal locus for photoswitch introduction (Figure 1).

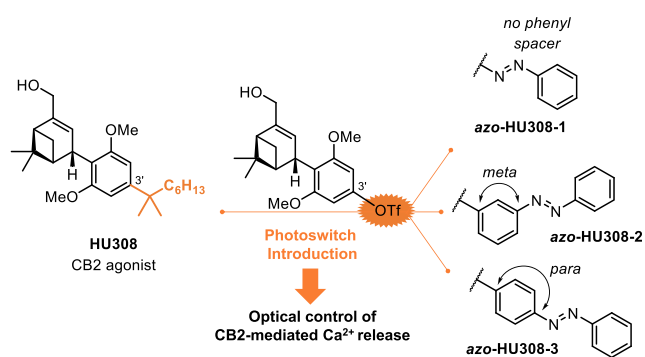
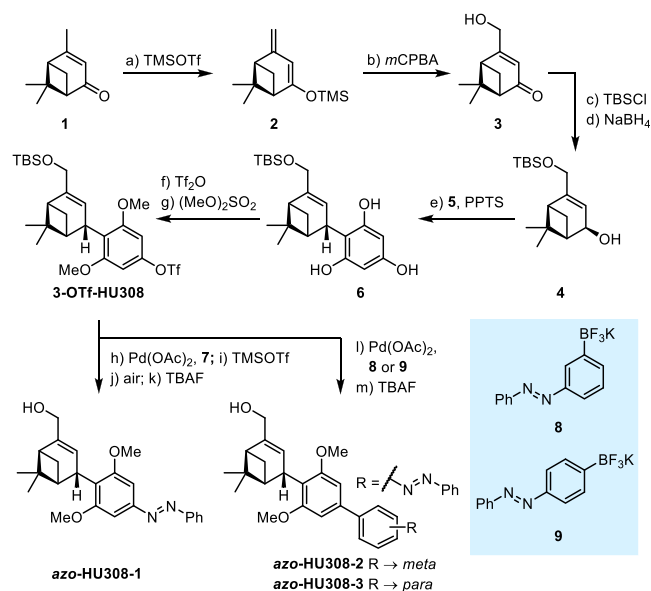


Figure 1. Photoswitchable *azo*-HU308 derivatives for optical control of CB2-mediated Ca^{2+} transients in AtT-20(CB2) cells.

Azobenzenes are presently the most prevalent switches in photopharmacology.³⁴ We devised three photoswitchable HU308 derivatives harboring azobenzenes. In *azo*-HU308-1, the phenyldiazene is directly attached to the resorcinylic core, whereas *azo*-HU308-2 and -3 include an additional phenyl spacer with *meta/para*-relationship between resorcinylic and diazene residues, respectively (Figure 1). At the heart of our retrosynthetic analysis is 3-OTf-HU308 as a common intermediate, which facilitates flexible late-stage azobenzene conjugation.

The synthesis of 3-OTf-HU308 commenced with the preparation of allylic alcohol **4** from (+)-verbenone (**1**), obtained in 62% yield by CrO_3 -mediated oxidation of (+)- α -pinene.³⁵ For the generation of γ -hydroxy verbenone **3**, we devised a vinylogous Rubottom oxidation of **1**.^{36,37} Treatment of **1** with Me_3SiOTf and *i*- Pr_2NET afforded corresponding silyl dienolether **2**, which was directly subjected to epoxidation using *m*CPBA under buffered conditions (Scheme 1).³⁸ Upon

Scheme 1. Synthesis of *azo*-HU308s⁴⁴



⁴⁴Reagents and conditions: (a) Me_3SiOTf , DIPEA, CH_2Cl_2 , 0 °C; (b) *m*CPBA, AcOH, py, CH_2Cl_2 , -25 °C, 62% over two steps; (c) *t*-Bu Me_2SiCl , NEt₃, DMAP, CH_2Cl_2 , rt, 83%; (d) NaBH₄, MeOH, rt, quantitative; (e) phloroglucinol (**5**), PPTS, MeCN, rt, 85%; (f) Tf_2O , 2,6-lutidine, CH_2Cl_2 , rt, 66%; (g) $(\text{MeO})_2\text{SO}_2$, K₂CO₃, acetone, 40 °C, 93%; (h) Pd(OAc)₂, *t*-Bu₃P-HBF₄, *N*-Boc-phenylhydrazine (**7**), Cs₂CO₃, toluene, 110 °C, 50%; (i) Me_3SiOTf , 2,6-lutidine, CH_2Cl_2 , 0 °C; (j) NaHCO₃, MeOH, air, rt, 89% over two steps; (k) Bu₄NF, THF, 0 °C to rt, 87%; (l) Pd(OAc)₂, PCy₃, Cs₂CO₃, **8** or **9**, THF/water, 70 °C; (m) Bu₄NF, THF, 0 °C to rt, 89% (*meta*), 94% (*para*) over two steps.

chromatographic purification on silica gel, γ -hydroxy verbenone **3** was obtained in 62% yield over 2 steps. This procedure for γ -oxidation proved more reliable and scalable than Wohl-Ziegler bromination followed by nucleophilic substitution.³² TBS-protection of the primary alcohol and stereoselective 1,2-reduction of the enone by NaBH₄ afforded pinene-derived allylic alcohol **4** in high yield.³⁹ The central C-C bond of the HU308 scaffold was then installed by Friedel-Crafts allylation of phloroglucinol (**5**) with **4**, employing PPTS to give **6** in 85% yield as a single diastereomer.^{40,41} Importantly, we found that the use of stoichiometric PPTS proved crucial for high yield. Excess phloroglucinol (10 equiv) suppressed overall allylation, and the use of solvent MeCN provides an alternative to per-silylation of phloroglucinol as reported by Makryannis and co-workers.^{42,43} *Para*-selective phenol triflation (Tf_2O , 2,6-lutidine) and bis-*O*-methylation with $(\text{MeO})_2\text{SO}_2$ afforded 3-OTf-HU308 in 66% yield over 2 steps. Finally, late stage derivatization was accomplished by means of cross-coupling chemistry. *Azo*-HU308-1 was accessed using a sequence of Buchwald-Hartwig coupling with *N*-Boc-phenylhydrazine (**7**), Boc-deprotection (Me_3SiOTf),⁴⁴ aerobic oxidation of the

diaryl-hydrazine, and deprotection of TBS ether (38% yield over 4 steps). *Azo*-HU308-2 and -3 were prepared via cross-coupling with corresponding potassium trifluoroborate reagents^{43,46} **8** and **9** under conditions reported by Molander and co-workers (Pd(OAc)₂, PCy₃, Cs₂CO₃, THF/water).⁴⁷ After TBS ether deprotection with Bu₄NF, *azo*-HU308-2 and -3 were obtained in excellent yields of 89 and 94% over 2 steps, respectively.

We proceeded to characterize the photophysical properties of *azo*-HU308s. In their resting state, they reside in the thermodynamically favored *trans*-configuration. Illumination at 365 nm (UV-A) leads to a photostationary state (PSS) favoring the *cis*-isomer. Irradiation at 455 nm (blue light) leads to a new PSS with *trans* as the dominant isomer (Figures 2, S1,

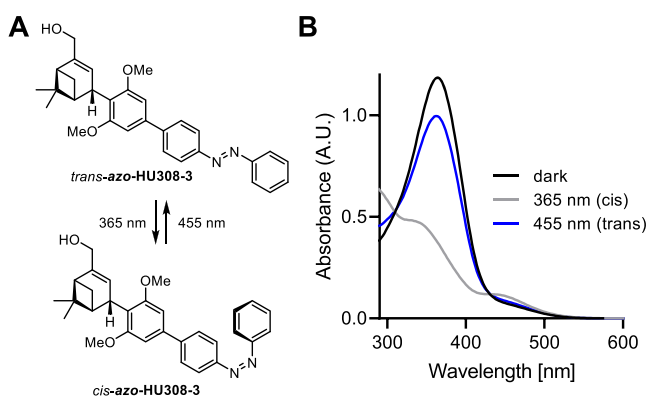


Figure 2. Photoisomerization of *azo*-HU308s. (A) *azo*-HU308-3 is isomerized between its *cis*- and *trans*-configurations with UV-A and blue irradiation, respectively. (B) UV-vis spectra of *azo*-HU308-3 (50 μ M in DMSO) in its dark-adapted (black), UV-A-adapted (gray), and blue light-adapted (blue) photostationary states.

and S2). *Trans*- and *cis*-isomer ratios at their photostationary states were quantified by HPLC analysis with UV detection at the isosbestic wavelengths. At 365 nm, *azo*-HU308-1-3 attain maximum *cis*-content of 80, 71, and 49%, respectively. Subsequently, at 455 nm, a new PSS is reached, with *trans*-content of 83, 86, and 87% (Figures S3 and S4). Additionally, *azo*-HU308s were moderately bistable, with *cis*-*azo*-HU308-1-3 relaxing to their *trans*-isomers with thermal half-lives ($t_{1/2}$ at rt and pH = 7) of 2.1, 6.5, and 1.6 h in H₂O, respectively (Figure S5).⁴⁸

Optical Control of Intracellular Ca²⁺ via CB2. A transformed mouse pituitary tumor AtT-20 cell line which stably expresses CB2 receptors (AtT-20(CB2) cells) reported by Mackie and co-workers was selected to explore the activity of the HU308-based photoswitches.⁴⁹ To confirm CB2 expression and membrane localization in this cell line, we utilized our recently reported HU308 derivative tagged with Alexa488 (Figure S6A).³³ This nonpermeable fluorescent probe binds specifically to CB2 receptors, and it allows real-time receptor visualization in living cells using fluorescence microscopy. For comparison, both AtT-20(CB2) and AtT-20-wild-type cells lacking CB2^{49,50} were incubated in parallel with fluoroprobe (150 nM) and nuclear stain Hoechst33342 (20 μ M). In AtT-20(CB2) cells, Alexa488-fluorescence was observed on the outer plasma membrane of most cells (Figure 3A, white arrows; Figure S6B, top), confirming that CB2 is expressed on the cell surface. We did not observe plasma membrane fluorescence in AtT-20-wild-type cells (Figure 3B;

Figure S6B, bottom), demonstrating the suitability of this fluorescent probe for specific visualization of CB2.

Classically, CB2 receptors are known to couple to G $\alpha_{i/o}$ proteins, which inhibit adenylyl cyclase activity.^{16,51,52} More recent studies suggest that CB2 can also couple to other G proteins and effector pathways.^{18,53} CB2 shows pronounced biased signaling on activation by different ligands, and the effects of CB2 activation on intracellular Ca²⁺ concentration ([Ca²⁺]_i) have only been described on few occasions.^{22–24,54–56} To the best of our knowledge, CB2-mediated modulation of [Ca²⁺]_i has not been reported for HU308 derivatives; therefore, we were intrigued to study Ca²⁺ signaling in living cells using HU308 and its photoswitchable derivatives. To assess the effect of HU308 in modulating CB2-mediated Ca²⁺ release, AtT-20(CB2) cells were loaded with Ca²⁺-sensitive Fluo-4-AM dye and subjected to real-time fluorescent Ca²⁺ imaging (Figure 3C).⁵⁷ Ionomycin (10 μ M), a Ca²⁺ ionophore that permeates cellular membranes, was added for normalization purposes at the end of the experiment. Upon the addition of HU308 (20 μ M), a large increase in Fluo-4 fluorescence intensity was observed, indicating that CB2 activation causes an increase in [Ca²⁺]_i (Figure 3C,D black, Figure S7A). Irradiation at 375 nm (UV-A) did not affect [Ca²⁺]_i before or after HU308 addition, confirming that light alone does not affect [Ca²⁺]_i in AtT-20(CB2) cells and that the effect of HU308 on [Ca²⁺]_i is not photosensitive. Lower concentrations of HU308 induced Ca²⁺ transients to a lesser degree (Figure S7B), and we determined an EC₅₀ of \sim 6.4 μ M (Figure S7C). As the binding affinity for HU308 is typically reported in the low nM range,³¹ this could indicate that this phenomenon is induced specifically at high CB2 receptor occupancies.⁵⁴

In control experiments, vehicle addition sometimes produced a small Ca²⁺ transient, which was not affected by irradiation (Figure S8A,B). Additionally, the effect of HU308 was substantially diminished in AtT-20-wild-type cells (Figure 3D, green), confirming the involvement of CB2 in initiating the Ca²⁺ response. The remaining small Ca²⁺ transient is likely an artifact by the mechanical force resulting from drug addition and was not blocked by the presence of CB2 inverse agonist AM630⁵⁸ (20 μ M) (Figure S8C).

Next, we investigated the effect of several CB2 antagonists/inverse agonists on the action of HU308 in AtT-20(CB2) cells (Figure 3E). In comparison to HU308 addition alone (20 μ M, black), SR144528⁵⁹ (20 μ M, blue) did not have a profound effect, while AM630 (20 μ M, green) dramatically reduced the Ca²⁺ transient. Interestingly, the addition of HU308 in the presence of JTE907⁶⁰ (40 μ M, red) resulted in a delayed and persistent Ca²⁺ transient. These results confirm the involvement of CB2 in driving this cellular response and highlight the intricacies of biased signaling mediated by a chemically diverse set of CB2 inverse agonists.

Cytosolic Ca²⁺ is known to originate from both extracellular matrix as well as various intracellular reservoirs, including endo/sarcoplasmic reticulum.²⁴ We thus sought to determine the mechanism by which HU308 and CB2 modulate [Ca²⁺]_i and to identify the source of the observed Ca²⁺ ions. First, Ca²⁺ in the extracellular imaging buffer was sequestered by addition of the chelator ethylene glycol-bis(2-aminoethyl ether)-N,N,N',N'-tetraacetic acid (EGTA, 0.1 mM), which prevents Ca²⁺ entry into the cell. Under these conditions, HU308 addition caused a rise in [Ca²⁺]_i of approximately the same magnitude; however, the effect subsided more rapidly when

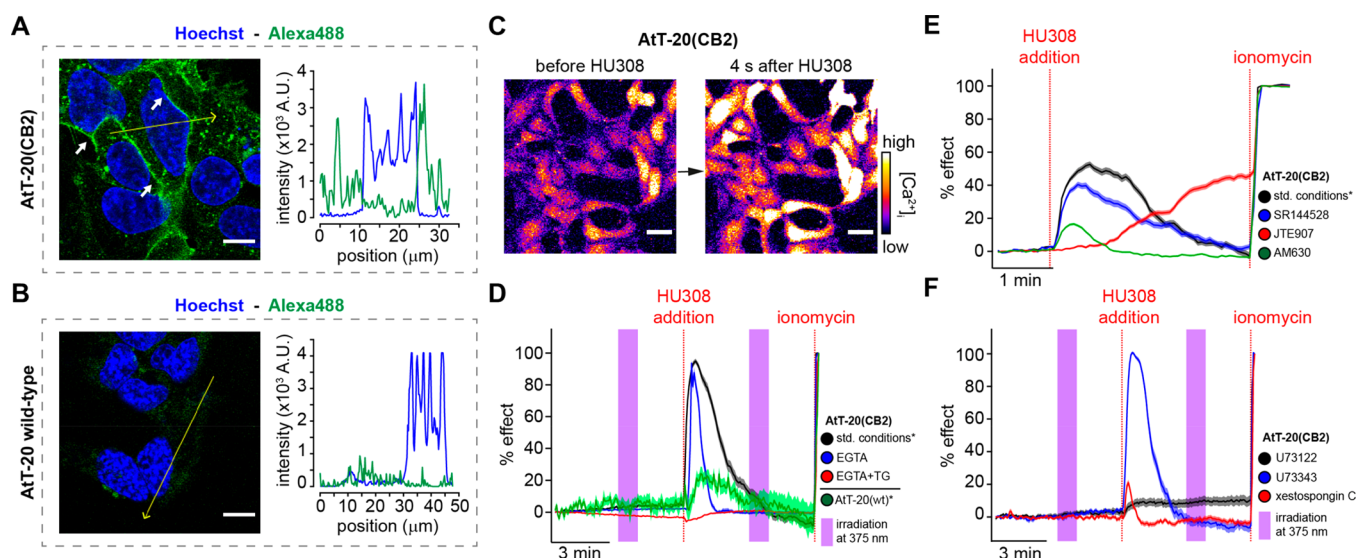


Figure 3. HU308 triggers Ca^{2+} transients in AtT-20(CB2) cells. Fluorescent labeling of CB2 using Alexa488-tagged HU308 derivative in (A) AtT-20(CB2) and (B) AtT-20-wild-type cells. Nuclei were stained with Hoechst33342 and white arrows highlight CB2 plasma membrane localization. Scale bars = 10 μm , right panels Intensity profile across the yellow line for Hoechst33342 and Alexa488 fluorescence. (C) Representative Ca^{2+} images using Fluo-4 dye reveals addition of HU308 (20 μM) increases Ca^{2+} levels in AtT-20(CB2) cells. Scale bars = 30 μm . (D) Average Fluo-4 intensity after addition of HU308 (20 μM) to AtT-20(CB2) cells under standard conditions (black, buffer containing 1.2 mM CaCl_2), after sequestration of extracellular Ca^{2+} (blue, $N = 100$, $T = 2$), and addition of thapsigargin (TG, 5 μM , red, $N = 100$, $T = 2$). The response to HU308 was sharply reduced in wild-type cells (green, $N = 100$, $T = 2$). (E) When compared to HU308 addition under standard conditions (black, $N = 463$, $T = 2$), AM630 (20 μM , green, $N = 754$, $T = 4$) blocked the Ca^{2+} transient. SR144528 (20 μM , blue, $N = 361$, $T = 2$) did not block the action of HU308, while JTE907 (40 μM , red, $N = 579$, $T = 3$) delayed the cellular response. (F) Co-application of PLC inhibitor U73122 (10 μM , black, $N = 99$, $T = 2$) blocked the effect of HU308 addition, while its inactive variant, U73343 (10 μM , black, $N = 100$, $T = 2$), did not. The IP₃ receptor antagonist xestospongin C (1 μM , red, $N = 150$, $T = 3$) also blocked the Ca^{2+} transient. Error bars = mean \pm s.e.m.

compared to experiments in the absence of EGTA (Figure 3D, blue). Cells were then pretreated with thapsigargin (5 μM), a sarco/endoplasmic reticulum Ca^{2+} -ATPase (SERCA) pump blocker. Thapsigargin alone did not block Ca^{2+} transients elicited by HU308 (Figure S8D). However, combination with EGTA for sequestration of extracellular Ca^{2+} completely abolished the effect of HU308 (Figure 3D, red). Finally, we probed the involvement of PLC in CB2-mediated $[\text{Ca}^{2+}]_i$ increase, which has previously been reported for endocannabinoids.²² The addition of PLC inhibitor U73122 (10 μM)⁶¹ greatly reduced the Ca^{2+} response induced by HU308 (Figure 3F, black). In control experiments, addition of the inactive U73122 analog, called U73343⁶¹ (10 μM), did not affect the response induced by HU308 (Figure 3F, blue). Finally, addition of IP₃-receptor antagonist xestospongin C⁶² (1 μM) greatly reduced Ca^{2+} transient (Figure 3F, red).

Taken together, these results suggest that HU308 stimulates Ca^{2+} release via CB2, $G\alpha_{q/11}$, and PLC in AtT-20(CB2) cells. We surmise that IP₃-receptor activation results in biphasic Ca^{2+} release from intracellular endo/sarcoplasmic reticulum Ca^{2+} stores, followed by activation of cell-surface Ca^{2+} channels. To the best of our knowledge, this represents a novel mechanism by which HU308 affects CB2 signaling at stimulatory GPCR effector pathways. These findings should be taken into account when employing this widely used benchmark ligand in pharmacological studies.

We set out to explore the possibility of exerting optical control over CB2-mediated Ca^{2+} transients. The three *azo*-HU308s were applied (each at 20 μM) to AtT20(CB2) cells loaded with Fluo-4 dye, and their effects on $[\text{Ca}^{2+}]_i$ were recorded before and after photoswitching. Most strikingly, *azo*-HU308-3 did not affect $[\text{Ca}^{2+}]_i$ prior to irradiation but did lead

to a sharp increase on irradiation at 375 nm, which suggests that only the *cis*-configuration has activity at CB2 (Figure 4A–C). After termination of irradiation, the Ca^{2+} increase subsided. Similar to that in experiments involving HU308, addition of PLC inhibitor U73122 (10 μM) or xestospongin C (1 μM) abolished the activity of *azo*-HU308-3 in either *trans*- or *cis*-form (Figure 4D, black and red, respectively). Although the response was reduced when compared to standard conditions, photoswitching was still observed in the presence of inactive PLC-inhibitor analog U73343 (10 μM) (Figure S9A). This confirms that *azo*-HU308-3, as HU308, affects Ca^{2+} transients in AtT-20(CB2) cells via PLC and IP₃ receptor signaling. Additionally, photoswitching was absent in AtT-20(CB2) cells in the presence of CB2 antagonist AM630 (20 μM) (Figure 4D, green) and in AtT-20-wild-type cells (Figure 4D, blue), which corroborates CB2 mediation. We were unable to observe photoswitching at lower concentrations (≤ 10 μM) of *azo*-HU308-3.

The other photoswitchable HU308 derivatives produced distinct effects on application and irradiation. In the case of *azo*-HU308-1, we observed a sharp increase in $[\text{Ca}^{2+}]_i$ on addition of the compound in its dark-adapted *trans*-configuration, and a $\sim 23\%$ decrease upon isomerization by irradiation at 375 nm (Figure 4C, Figure S9B). This suggests greater potency for *azo*-HU308-1 in the *trans*-configuration. In contrast, *azo*-HU308-2 showed no effect on $[\text{Ca}^{2+}]_i$ in either the *trans*- or *cis*-form at 20 μM (Figure 4C, Figure S9C). Together, these results confirm that, among all *azo*-HU308s, *azo*-HU308-3 is the best for manipulating CB2 with light through a mechanism identical to its parent compound. Importantly, our findings demonstrate for the first time optical control over CB2-mediated Ca^{2+} -transients.

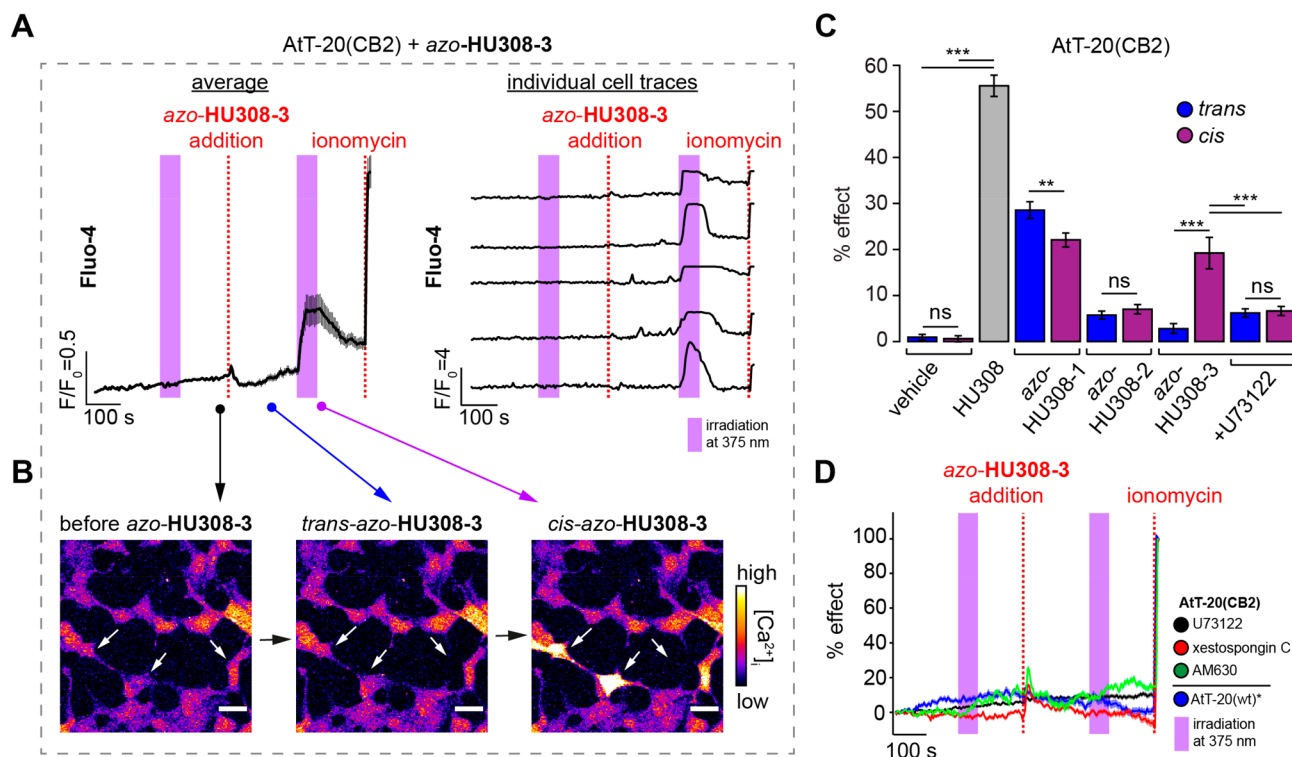


Figure 4. Azo-HU308s control Ca^{2+} transient in AtT-20(CB2) cells. (A) Averaged (left) and single cell (right) Ca^{2+} imaging traces with Fluo-4 for azo-HU308-3 (20 μM , $N = 65$, $T = 2$) showing an increase in Ca^{2+} induced by azo-HU308-3. (B) Representative fluorescence images (scale bar = 30 μm). (C) Summary bar graph for Ca^{2+} assay comparing vehicle ($N = 80$, $T = 2$), HU308 (20 μM , $N = 100$, $T = 2$), azo-HU308-1 (20 μM , $N = 150$, $T = 3$), azo-HU308-2 (20 μM , $N = 60$, $T = 2$), azo-HU308-3 (20 μM , $N = 65$, $T = 2$) and azo-HU308-3 + U73112 (10 μM , $N = 100$) in *trans* (blue) and *cis* configuration (purple). (D) Incubating AtT-20(CB2) cells with U73112 (10 μM , black, $N = 100$, $T = 2$), xestospongin C (red, 1 μM , $N = 150$, $T = 3$), or AM630 (20 μM , green, $N = 100$, $T = 2$) abolished the effect of azo-HU308-3 (20 μM). The effect of azo-HU308-3 was not present in AtT-20 wild-type cells (blue, $N = 100$, $T = 2$). Error bars = mean \pm s.e.m. * $P < 0.05$, ** $P < 0.01$, *** $P < 0.001$, ns = not significant.

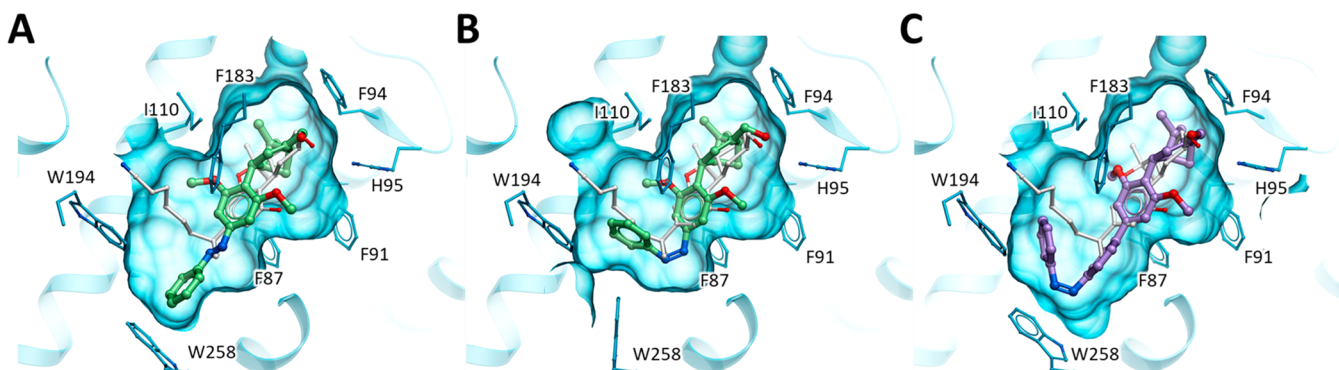


Figure 5. Predicted docking poses for (A) *trans*-azo-HU308-1, (B) *cis*-azo-HU308-1, and (C) *cis*-azo-HU308-3 employing CB2 cocystal structure with agonist AM12033 (PDB ID: 6kpc). *Trans*-azo-HU308-3 is not shown as *cis*-to-*trans* switch results in major clash with the receptor, which prevents reasonable docking. The receptor pocket is represented in blue sticks and transparent shape, and the cocrystallized ligand AM12033 is shown in white. The predicted docking poses of azo-HU308-1 are shown in green, and of azo-HU308-3 in purple.

Molecular Modeling and Docking. Flexible docking of HU308 and its azo-derivatives was performed with the structure of CB2 solved as cocystal with agonist AM12033 (3.2 \AA resolution).¹⁶ To account for minor flexibility in the binding pocket, the conformations of receptor amino acid side chains within 8 \AA radius from the ligands were co-optimized alongside ligand conformation. To establish the baseline values for the prediction of ligand binding poses and scores, we performed the redocking of cocrystallized agonist AM12033, as well as HU308 (Figure S10). The predicted docking pose of AM12033 showed strong agreement with the cocystal

structure (RMSD = 0.39 \AA) and high docking score (−35 kJ/mol). The pose of HU308 overlapped with AM12033 in the common parts of the scaffolds and produced a comparable docking score (−30 kJ/mol).

Docking poses and scores were predicted for *cis*- and *trans*-isomers of each azo-HU308 (Table S1). The results show that all three active isomers, *trans*-azo-HU308-1, *cis*-azo-HU308-1, and *cis*-azo-HU-308-3, have docking scores of −27, −26, and −26 kJ/mol, respectively. Although these are still favorable binding scores, these values are ~3–4 kJ/mol lower than for HU308. This result is consistent with our experimental

observations that the photoswitchable derivatives are less potent at triggering CB2-mediated Ca^{2+} transients than the parent compound. The *in silico* binding poses for the resorcinyln-pinenyl core are similar to the predicted orientation of HU308. Their azobenzene residues extend into the deep part of the hydrophobic binding pocket (Figure 5). *Trans-azo-HU308-3*, with its more extended configuration, failed to fit into the CB2 binding pocket, as it clashes with W258^{6,48}. Both *trans*- and *cis-azo-HU308-2* isomers docked with inferior binding scores (−13 and −16 kJ/mol, respectively) and with predicted poses that were dramatically distorted from that of HU308 (Figure S11). This corroborates their lack of activity in the Ca^{2+} fluorescence assay. Interestingly, we observed that in order to accommodate the azobenzene substituent of some *azo*-HU308s (e.g., *trans-azo-HU308-1* and *cis-azo-HU308-3*), the side chain of W258^{6,48} rotates about 30° without causing any substantial change in the surrounding residues (Figure S12). This result suggests that the active state of CB2 has some flexibility in the orientation of W258^{6,48} side chain, which represents a highly conserved toggle switch in class A GPCRs and has a crucial role in GPCR activation.¹⁷

CONCLUSION

We report for the first time that the commonly employed CB2 agonist HU308 stimulates CB2/PLC-mediated Ca^{2+} flux in AtT-20(CB2) cells. Photoswitchable derivatives of HU308 were designed and studied to control CB2-mediated cellular excitability through $[\text{Ca}^{2+}]_i$. Late-stage diversification of building block 3-OTf-HU308 gave rise to azobenzene-containing HU308 derivatives. These *azo*-HU308s enable optical control over Ca^{2+} levels in AtT-20(CB2) cells with spatiotemporal precision. Importantly, the complementary behavior of *azo-HU308-1* and *azo-HU308-3* (i.e., *trans* vs *cis*-active) will be useful in the design of experiments to manipulate CB2 in a wide range of physiological arenas. *In silico* docking studies validated our experimental findings on the structural dependence of CB2 activity. We anticipate the use of this structural information for the design of additional photoswitchable CB2 ligands with the bespoke photophysical and pharmacological properties. For example, these may include red-shifted photochromic derivatives for use in intact tissue or *in vivo*.

HU308 has been used in the study of numerous CB2-mediated effector pathways. In order to fully realize the potential of *azo*-HU308s, studies toward optical control of other CB2 signaling pathways, including adenylyl cyclase, β -arrestin, and ERK1/2, are currently underway in our laboratories. In combination with additional investigations which apply the *azo*-HU308s to cells that express CB2 endogenously, our efforts will reveal the unique mechanisms by which *azo*-HU308s affect CB2 biased signaling pathways in different physiological settings. As novel tools to precisely control CB2 signaling, *azo*-HU308s will find applications in complex physiological settings, thereby enhancing understanding of CB2, in particular, and, more broadly, cannabinoid chemistry and biology.

ASSOCIATED CONTENT

Supporting Information

The Supporting Information is available free of charge at <https://pubs.acs.org/doi/10.1021/jacs.0c08926>.

Detailed experimental methods and compound characterization (PDF)

AUTHOR INFORMATION

Corresponding Authors

James A. Frank – Vollum Institute, Oregon Health & Science University, Portland, Oregon 97239-3098, United States; orcid.org/0000-0001-6705-2540; Email: frankja@ohsu.edu

Erick M. Carreira – Laboratorium für Organische Chemie, Eidgenössische Technische Hochschule Zürich, 8093 Zürich, Switzerland; orcid.org/0000-0003-1472-490X; Email: erickm.carreira@org.chem.ethz.ch

Authors

Roman C. Sarott – Laboratorium für Organische Chemie, Eidgenössische Technische Hochschule Zürich, 8093 Zürich, Switzerland; orcid.org/0000-0001-8789-6150

Alexander E. G. Viray – Vollum Institute, Oregon Health & Science University, Portland, Oregon 97239-3098, United States

Patrick Pfaff – Laboratorium für Organische Chemie, Eidgenössische Technische Hochschule Zürich, 8093 Zürich, Switzerland; orcid.org/0000-0002-9761-2497

Anastasiia Sadybekov – Department of Quantitative and Computational Biology and Department of Chemistry, Bridge Institute, University of Southern California, Los Angeles, California 90089, United States

Gabriela Rajic – Vollum Institute, Oregon Health & Science University, Portland, Oregon 97239-3098, United States

Vsevolod Katritch – Department of Quantitative and Computational Biology and Department of Chemistry, Bridge Institute, University of Southern California, Los Angeles, California 90089, United States; orcid.org/0000-0003-3883-4505

Complete contact information is available at:

<https://pubs.acs.org/10.1021/jacs.0c08926>

Funding

E.M.C gratefully acknowledges support by ETH Zürich. R.C.S and P.P. gratefully acknowledge funding from the Scholarship Fund of the Swiss Chemical Industry (SSCI). J.A.F., A.E.G.V., and G.R. acknowledge the Vollum Institute Fellowship for financial support.

Notes

The authors declare no competing financial interest.

ACKNOWLEDGMENTS

We thank Ken Mackie for providing AtT-20 cell lines reagents and for helpful discussions and Carsten Schultz for providing access to microscopy resources. Dr. Matthias V. Westphal and Dr. Michael A. Schafroth are gratefully acknowledged for helpful discussions.

REFERENCES

- (1) Pacher, P.; Kunos, G. Modulating the Endocannabinoid System in Human Health and Disease—Successes and Failures. *FEBS J.* **2013**, *280*, 1918.
- (2) Han, S.; Thatte, J.; Buzard, D. J.; Jones, R. M. Therapeutic Utility of Cannabinoid Receptor Type 2 (CB2) Selective Agonists. *J. Med. Chem.* **2013**, *56*, 8224.

- (3) Marzo, V. D.; Bifulco, M.; Petrocellis, L. D. The Endocannabinoid System and Its Therapeutic Exploitation. *Nat. Rev. Drug Discovery* **2004**, *3*, 771.
- (4) Maccarrone, M.; Bab, I.; Bíró, T.; Cabral, G. A.; Dey, S. K.; Di Marzo, V.; Konje, J. C.; Kunos, G.; Mechoulam, R.; Pacher, P.; Sharkey, K. A.; Zimmer, A. Endocannabinoid Signaling at the Periphery: 50 Years after THC. *Trends Pharmacol. Sci.* **2015**, *36*, 277.
- (5) Matsuda, L. A.; Lolait, S. J.; Brownstein, M. J.; Young, A. C.; Bonner, T. I. Structure of a Cannabinoid Receptor and Functional Expression of the Cloned cDNA. *Nature* **1990**, *346*, 561.
- (6) Gaoni, Y.; Mechoulam, R. Isolation, Structure, and Partial Synthesis of an Active Constituent of Hashish. *J. Am. Chem. Soc.* **1964**, *86*, 1646.
- (7) Mechoulam, R. *Marijuana: Chemistry, Pharmacology, Metabolism and Clinical Effects*; Academic Press: 1973.
- (8) Galiègue, S.; Mary, S.; Marchand, J.; Dussossoy, D.; Carrière, D.; Carayon, P.; Bouaboula, M.; Shire, D.; Le Fur, G.; Casellas, P. Expression of Central and Peripheral Cannabinoid Receptors in Human Immune Tissues and Leukocyte Subpopulations. *Eur. J. Biochem.* **1995**, *232*, 54.
- (9) Munro, S.; Thomas, K. L.; Abu-Shaar, M. Molecular Characterization of a Peripheral Receptor for Cannabinoids. *Nature* **1993**, *365*, 61.
- (10) Turcotte, C.; Blanchet, M.-R.; Laviolette, M.; Flamand, N. The CB2 Receptor and Its Role as a Regulator of Inflammation. *Cell. Mol. Life Sci.* **2016**, *73*, 4449.
- (11) Guindon, J.; Hohmann, A. G. Cannabinoid CB2 Receptors: A Therapeutic Target for the Treatment of Inflammatory and Neuropathic Pain. *Br. J. Pharmacol.* **2008**, *153*, 319.
- (12) Dhopeswarkar, A.; Mackie, K. CB2 Cannabinoid Receptors as a Therapeutic Target—What Does the Future Hold? *Mol. Pharmacol.* **2014**, *86*, 430.
- (13) Pacher, P.; Mechoulam, R. Is Lipid Signaling through Cannabinoid 2 Receptors Part of a Protective System? *Prog. Lipid Res.* **2011**, *50*, 193.
- (14) Shoemaker, J. L.; Seely, K. A.; Reed, R. L.; Crow, J. P.; Prather, P. L. The CB2 Cannabinoid Agonist AM-1241 Prolongs Survival in a Transgenic Mouse Model of Amyotrophic Lateral Sclerosis When Initiated at Symptom Onset. *J. Neurochem.* **2007**, *101*, 87.
- (15) Li, X.; Hua, T.; Vemuri, K.; Ho, J.-H.; Wu, Y.; Wu, L.; Popov, P.; Benchama, O.; Zvonok, N.; Locke, K.; Qu, L.; Han, G. W.; Iyer, M. R.; Cinar, R.; Coffey, N. J.; Wang, J.; Wu, M.; Katritch, V.; Zhao, S.; Kunos, G.; Bohn, L. M.; Makriyannis, A.; Stevens, R. C.; Liu, Z.-J. Crystal Structure of the Human Cannabinoid Receptor CB2. *Cell* **2019**, *176* (3), 459.
- (16) Hua, T.; Li, X.; Wu, L.; Iliopoulos-Tsoutsouvas, C.; Wang, Y.; Wu, M.; Shen, L.; Johnston, C. A.; Nikas, S. P.; Song, F.; Song, X.; Yuan, S.; Sun, Q.; Wu, Y.; Jiang, S.; Grim, T. W.; Benchama, O.; Stahl, E. L.; Zvonok, N.; Zhao, S.; Bohn, L. M.; Makriyannis, A.; Liu, Z.-J. Activation and Signaling Mechanism Revealed by Cannabinoid Receptor-Gi Complex Structures. *Cell* **2020**, *180*, 655.
- (17) Xing, C.; Zhuang, Y.; Xu, T.-H.; Feng, Z.; Zhou, X. E.; Chen, M.; Wang, L.; Meng, X.; Xue, Y.; Wang, J.; Liu, H.; McGuire, T. F.; Zhao, G.; Melcher, K.; Zhang, C.; Xu, H. E.; Xie, X.-Q. Cryo-EM Structure of the Human Cannabinoid Receptor CB2-Gi Signaling Complex. *Cell* **2020**, *180*, 645–654.
- (18) Saroz, Y.; Kho, D. T.; Glass, M.; Graham, E. S.; Grimsey, N. L. Cannabinoid Receptor 2 (CB2) Signals via G-Alpha-s and Induces IL-6 and IL-10 Cytokine Secretion in Human Primary Leukocytes. *ACS Pharmacol. Transl. Sci.* **2019**, *2*, 414.
- (19) Soethoudt, M.; Grether, U.; Fingerle, J.; Grim, T. W.; Fezza, F.; de Petrocellis, L.; Ullmer, C.; Rothenhausler, B.; Perret, C.; van Gils, N.; Finlay, D.; MacDonald, C.; Chicca, A.; Gens, M. D.; Stuart, J.; de Vries, H.; Mastrangelo, N.; Xia, L.; Alachouzou, G.; Baggelaar, M. P.; Martella, A.; Mock, E. D.; Deng, H.; Heitman, L. H.; Connor, M.; Di Marzo, V.; Gertsch, J.; Lichtman, A. H.; Maccarrone, M.; Pacher, P.; Glass, M.; van der Stelt, M. Cannabinoid CB₂ Receptor Ligand Profiling Reveals Biased Signalling and off-Target Activity. *Nat. Commun.* **2017**, *8*, 13958.
- (20) Bezprozvanny, I. Calcium Signaling and Neurodegenerative Diseases. *Trends Mol. Med.* **2009**, *15*, 89.
- (21) LaFerla, F. M. Calcium Dyshomeostasis and Intracellular Signalling in Alzheimer's Disease. *Nat. Rev. Neurosci.* **2002**, *3*, 862.
- (22) Zoratti, C.; Kipmen-Korgun, D.; Osibow, K.; Malli, R.; Graier, W. F. Anandamide Initiates Ca²⁺ Signaling via CB2 Receptor Linked to Phospholipase C in Calf Pulmonary Endothelial Cells. *R. J. Pharmacol.* **2003**, *140*, 1351.
- (23) Juan-Picó, P.; Fuentes, E.; Javier Bermúdez-Silva, F.; Javier Díaz-Molina, F.; Ripoll, C.; Rodríguez de Fonseca, F.; Nadal, A. Cannabinoid Receptors Regulate Ca²⁺ Signals and Insulin Secretion in Pancreatic β -Cell. *Cell Calcium* **2006**, *39*, 155.
- (24) Brailoiu, G. C.; Deliu, E.; Marcu, J.; Hoffman, N. E.; Console-Bram, L.; Zhao, P.; Madesh, M.; Abood, M. E.; Brailoiu, E. Differential Activation of Intracellular versus Plasmalemmal CB2 Cannabinoid Receptors. *Biochemistry* **2014**, *53*, 4990.
- (25) Velema, W. A.; Szymanski, W.; Feringa, B. L. Photopharmacology: Beyond Proof of Principle. *J. Am. Chem. Soc.* **2014**, *136*, 2178.
- (26) Hüll, K.; Morstein, J.; Trauner, D. In Vivo Photopharmacology. *Chem. Rev.* **2018**, *118*, 10710–10747.
- (27) For a recent example of non-CB2-mediated optical control over [Ca]_i, see Yang, X.; Ma, G.; Zheng, S.; Qin, X.; Li, X.; Du, L.; Wang, Y.; Zhou, Y.; Li, M. Optical Control of CRAC Channels Using Photoswitchable Azopyrazoles. *J. Am. Chem. Soc.* **2020**, *142*, 9460.
- (28) Westphal, M. V.; Schafroth, M. A.; Sarott, R. C.; Imhof, M. A.; Bold, C. P.; Leippe, P.; Dhopeswarkar, A.; Grandner, J. M.; Katritch, V.; Mackie, K.; Trauner, D.; Carreira, E. M.; Frank, J. A. Synthesis of Photoswitchable Δ^9 -Tetrahydrocannabinol Derivatives Enables Optical Control of Cannabinoid Receptor 1 Signaling. *J. Am. Chem. Soc.* **2017**, *139*, 18206.
- (29) For more examples of optical control of GPCRs by means of photopharmacology, see: (a) Hauwert, N. J.; Mocking, T. A. M.; Da Costa Pereira, D.; Kooistra, A. J.; Wijnen, L. M.; Vreeker, G. C. M.; Verweij, E. W. E.; De Boer, A. H.; Smit, M. J.; De Graaf, C.; Vischer, H. F.; de Esch, I. J. P.; Wijnmans, M.; Leurs, R. Synthesis and Characterization of a Bidirectional Photoswitchable Antagonist Toolbox for Real-Time GPCR Photopharmacology. *J. Am. Chem. Soc.* **2018**, *140*, 4232. (b) Hauwert, N. J.; Mocking, T. A. M.; Da Costa Pereira, D.; Lion, K.; Huppelschoten, Y.; Vischer, H. F.; De Esch, I. J. P.; Wijnmans, M.; Leurs, R. A Photoswitchable Agonist for the Histamine H₃ Receptor, a Prototypic Family A G-Protein-Coupled Receptor. *Angew. Chem., Int. Ed.* **2019**, *58*, 4531. (c) Pittolo, S.; Lee, H.; Lladó, A.; Tosi, S.; Bosch, M.; Bardia, L.; Gómez-Santacana, X.; Llebaria, A.; Soriano, E.; Colombelli, J.; Poskanzer, K. E.; Perea, G.; Gorostiza, P. Reversible Silencing of Endogenous Receptors in Intact Brain Tissue using 2-Photon Pharmacology. *Proc. Natl. Acad. Sci. U. S. A.* **2019**, *116*, 13680.
- (30) Dolles, D.; Strasser, A.; Wittmann, H.-J.; Marinelli, O.; Nabissi, M.; Pertwee, R. G.; Decker, M. The First Photochromic Affinity Switch for the Human Cannabinoid Receptor 2. *Adv. Therap.* **2018**, *1*, 1700032.
- (31) Hanuš, L.; Breuer, A.; Tchilibon, S.; Shiloah, S.; Goldenberg, D.; Horowitz, M.; Pertwee, R. G.; Ross, R. A.; Mechoulam, R.; Fride, E. HU-308: A Specific Agonist for CB2, a Peripheral Cannabinoid Receptor. *Proc. Natl. Acad. Sci. U. S. A.* **1999**, *96*, 14228.
- (32) Westphal, M. V.; Sarott, R. C.; Zirwes, E. A.; Osterwald, A.; Guba, W.; Ullmer, C.; Grether, U.; Carreira, E. M. Highly Selective, Amine-Derived Cannabinoid Receptor 2 Probes. *Chem. Eur. J.* **2020**, *26*, 1380.
- (33) Sarott, R. C.; Westphal, M. V.; Pfaff, P.; Korn, C.; Sykes, D. A.; Gazi, T.; Brennecke, B.; Atz, K.; Weise, M.; Mostinski, Y.; Hompluem, P.; Koers, E.; Miljus, T.; Roth, N. J.; Asmellash, H.; Vong, M. C.; Piovesan, J.; Guba, W.; Rufer, A. C.; Kuszniar, E. A.; Huber, S.; Raposo, C.; Zirwes, E. A.; Osterwald, A.; Pavlovic, A.; Moes, S.; Beck, J.; Benito-Cuesta, I.; Grande, T.; Ruiz de Martín Esteban, S.; Yeliseev, A.; Drawnel, F.; Widmer, G.; Holzer, D.; van der Wel, T.; Mandhair, H.; Yuan, C.-Y.; Drobyski, W. R.; Saroz, Y.; Grimsey, N.; Honer, M.; Fingerle, J.; Gawrisch, K.; Romero, J.;

- Hillard, C. J.; Varga, Z. V.; van der Stelt, M.; Pacher, P.; Gertsch, J.; McCormick, P. J.; Ullmer, C.; Oddi, S.; Maccarrone, M.; Veprincev, D. B.; Nazare, M.; Grether, U.; Carreira, E. M. Development of High-Specificity Fluorescent Probes to Enable Cannabinoid Type 2 Receptor Studies in Living Cells. *J. Am. Chem. Soc.* **2020**, *142*, 16953.
- (34) Broichhagen, J.; Frank, J. A.; Trauner, D. A Roadmap to Success in Photopharmacology. *Acc. Chem. Res.* **2015**, *48*, 1947.
- (35) Marwah, P.; Lardy, H. A. Process for Effecting Allylic Oxidation Using Dicarboxylic Acid Imides and Chromium Reagents. US6384251 B1, May 7, 2002.
- (36) Gondi, V. B.; Loch, J. T. I.; Holman, N. J.; Collier, S. J. Process for the Preparation of 3-Substituted Cannabinoid Compounds. Patent WO2017093749, June 8, 2017.
- (37) Fujiwara, H.; Kurogi, T.; Okaya, S.; Okano, K.; Tokuyama, H. Total Synthesis of (–)-Acetylarnotin. *Angew. Chem., Int. Ed.* **2012**, *51*, 13062.
- (38) Wang, H.; Andemichael, Y. W.; Vogt, F. G. A Scalable Synthesis of 2S-Hydroxymutilin via a Modified Rubottom Oxidation. *J. Org. Chem.* **2009**, *74*, 478.
- (39) Mechoulam, R.; Lander, N.; University, A.; Zahalka, J. Synthesis of the Individual, Pharmacologically Distinct, Enantiomers of a Tetrahydrocannabinol Derivative. *Tetrahedron: Asymmetry* **1990**, *1*, 315.
- (40) Hoffmann, G.; Daniliuc, C. G.; Studer, A. Synthesis of Para (–)- Δ^8 -THC Triflate as a Building Block for the Preparation of THC Derivatives Bearing Different Side Chains. *Org. Lett.* **2019**, *21*, 563.
- (41) We have found that the use phloroglucinol (**5**) as nucleophile prevented formation of undesired regioisomeric adduct, as observed for 3-bromoresorcinol in: Hoffmann, G.; Studer, A. Short and Protecting-Group-Free Approach to the (–)- Δ^8 -THC-Motif: Synthesis of THC-Analogues, (–)-Machaeriol B and (–)-Machaeriol D. *Org. Lett.* **2018**, *20*, 2964.
- (42) Dixon, D. D.; Sethumadhavan, D.; Benneche, T.; Banaag, A. R.; Tius, M. A.; Thakur, G. A.; Bowman, A.; Wood, J. T.; Makriyannis, A. Heteroadamantyl Cannabinoids. *J. Med. Chem.* **2010**, *53*, 5656.
- (43) Dixon, D. D.; Tius, M. A.; Thakur, G. A.; Zhou, H.; Bowman, A. L.; Shukla, V. G.; Peng, Y.; Makriyannis, A. C3-Heteroaroyl Cannabinoids as Photolabeling Ligands for the CB2 Cannabinoid Receptor. *Bioorg. Med. Chem. Lett.* **2012**, *22*, 5322.
- (44) Bastiaans, H. M. M.; van der Baan, J. L.; Ottenheijm, H. C. J. Flexible and Convergent Total Synthesis of Cyclotheonamide B. *J. Org. Chem.* **1997**, *62*, 3880.
- (45) Harvey, J. H.; Butler, B. K.; Trauner, D. Functionalized Azobenzenes through Cross-Coupling with Organotrifluoroborates. *Tetrahedron Lett.* **2007**, *48*, 1661.
- (46) Darses, S.; Michaud, G.; Genêt, J.-P. Potassium Organo-trifluoroborates: New Partners in Palladium-Catalysed Cross-Coupling Reactions. *Eur. J. Org. Chem.* **1999**, *1999*, 1875.
- (47) Molander, G. A.; Petrillo, D. E.; Landzberg, N. R.; Rohanna, J. C.; Biolatto, B. Palladium-Catalyzed Suzuki-Miyaura Reactions of Potassium Aryl- and Heteroaryltrifluoroborates with Aryl- and Heteroaryl Triflates. *Synlett* **2005**, *2005*, 1763.
- (48) Ahmed, Z.; Siiskonen, A.; Virkki, M.; Priimagi, A. Controlling Azobenzene Photoswitching through Combined Ortho-Fluorination and -Amination. *Chem. Commun.* **2017**, *53*, 12520.
- (49) Atwood, B. K.; Wager-Miller, J.; Haskins, C.; Straiker, A.; Mackie, K. Functional Selectivity in CB(2) Cannabinoid Receptor Signaling and Regulation: Implications for the Therapeutic Potential of CB(2) Ligands. *Mol. Pharmacol.* **2012**, *81*, 250.
- (50) Felder, C. C.; Joyce, K. E.; Briley, E. M.; Mansouri, J.; Mackie, K.; Blond, O.; Lai, Y.; Ma, A. L.; Mitchell, R. L. Comparison of the Pharmacology and Signal Transduction of the Human Cannabinoid CB1 and CB2 Receptors. *Mol. Pharmacol.* **1995**, *48*, 443.
- (51) Howlett, A. C.; Barth, F.; Bonner, T. I.; Cabral, G.; Casellas, P.; Devane, W. A.; Felder, C. C.; Herkenham, M.; Mackie, K.; Martin, B. R.; Mechoulam, R.; Pertwee, R. G. International Union of Pharmacology. XXVII. Classification of Cannabinoid Receptors. *Pharmacol. Rev.* **2002**, *54*, 161.
- (52) Demuth, D. G.; Molleman, A. Cannabinoid Signalling. *Life Sci.* **2006**, *78*, 549.
- (53) Viscomi, M. T.; Oddi, S.; Latini, L.; Pasquariello, N.; Florenzano, F.; Bernardi, G.; Molinari, M.; Maccarrone, M. Selective CB2 Receptor Agonism Protects Central Neurons from Remote Axotomy-Induced Apoptosis through the PI3K/Akt Pathway. *J. Neurosci.* **2009**, *29*, 4564.
- (54) Shoemaker, J. L.; Ruckle, M. B.; Mayeux, P. R.; Prather, P. L. Agonist-Directed Trafficking of Response by Endocannabinoids Acting at CB2 Receptors. *J. Pharmacol. Exp. Ther.* **2005**, *315*, 828.
- (55) Rao, G. K.; Kaminski, N. E. Cannabinoid-Mediated Elevation of Intracellular Calcium: A Structure-Activity Relationship. *J. Pharmacol. Exp. Ther.* **2006**, *317*, 820.
- (56) Sugiura, T.; Kondo, S.; Kishimoto, S.; Miyashita, T.; Nakane, S.; Kodaka, T.; Sahara, Y.; Takayama, H.; Waku, K. Evidence That 2-Arachidonoylglycerol but Not N-Palmitoylethanolamine or Anandamide Is the Physiological Ligand for the Cannabinoid CB2 Receptor. Comparison of the Agonistic Activities of various Cannabinoid Ligands in HL-60 Cells. *J. Biol. Chem.* **2000**, *275*, 605.
- (57) Tovey, S. C.; Sun, Y.; Taylor, C. W. Rapid Functional Assays of Intracellular Ca²⁺ Channels. *Nat. Protoc.* **2006**, *1*, 259.
- (58) Ross, R. A.; Brockie, H. C.; Stevenson, L. A.; Murphy, V. L.; Templeton, F.; Makriyannis, A.; Pertwee, R. G. Agonist-Inverse Agonist Characterization at CB1 and CB2 Cannabinoid Receptors of L759633, L759656 and AM630. *Br. J. Pharmacol.* **1999**, *126*, 665.
- (59) Rinaldi-Carmona, M.; Barth, F.; Millan, J.; Derocq, J.-M.; Casellas, P.; Congy, C.; Oustric, D.; Sarran, M.; Bouaboula, M.; Calandra, B.; Portier, M.; Shire, D.; Brelière, J.-C.; Fur, G. L. SR 144528, the First Potent and Selective Antagonist of the CB2 Cannabinoid Receptor. *J. Pharmacol. Exp. Ther.* **1998**, *284*, 644.
- (60) Iwamura, H.; Suzuki, H.; Ueda, Y.; Kaya, T.; Inaba, T. In Vitro and in Vivo Pharmacological Characterization of JTE-907, a Novel Selective Ligand for Cannabinoid CB2 Receptor. *J. Pharmacol. Exp. Ther.* **2001**, *296*, 420.
- (61) Bleasdale, J. E.; Thakur, N. R.; Gremban, R. S.; Bundy, G. L.; Fitzpatrick, F. A.; Smith, R. J.; Bunting, S. Selective Inhibition of Receptor-Coupled Phospholipase C-Dependent Processes in Human Platelets and Polymorphonuclear Neutrophils. *J. Pharmacol. Exp. Ther.* **1990**, *255*, 756.
- (62) Gafni, J.; Munsch, J. A.; Lam, T. H.; Catlin, M. C.; Costa, L. G.; Molinski, T. F.; Pessah, I. N. Xestospingins: Potent Membrane Permeable Blockers of the Inositol 1,4,5-Trisphosphate Receptor. *Neuron* **1997**, *19*, 723.